CTH-RF-103, April 1994

Detailed Monte Carlo simulation of electron elastic scattering

by

R. Chakarova

CTH-RF-103, April 1994

Detailed Monte Carlo simulation of electron elastic scattering

by

R. Chakarova

Department of Reactor Physics
Chalmers University of Technology
S - 412 96 Göteborg,Sweden
ISSN 0281-9775

Detailed Monte Carlo simulation of electron elastic scattering

by

R. Chakarova

Department of Reactor Physics
Chalmers University of Technology
S-41296 Göteborg, Sweden

Abstract

A detailed Monte Carlo model is described which simulates the transport of electrons penetrating a medium without energy loss. The trajectory of each electron is constructed as a series of successive interaction events - elastic or inelastic scattering. Differential elastic scattering cross sections, elastic and inelastic mean free paths are used to describe the interaction process. It is presumed that the cross sections data are available and the Monte Carlo algorithm does not include their evaluation. Electrons suffering successive elastic collisions are followed until they escape from the medium or (if the absorption is negligible) their path length exceeds a certain value. The inelastic events are thus treated as absorption.

The medium geometry is a layered infinite slab. The electron source could be an incident electron beam or electrons created inside the material.

The objective is to obtain the angular distribution, the path length and depth distribution and the collision number distribution of electrons emitted through the surface of the medium.

The model is applied successfully to electrons with energy between 0.4 and 2.1 keV reflected from semi - infinite homogeneous materials with different scattering properties.

CONTENTS

1. INTRODUCTION

1.1. Condensed and detailed Monte Carlo simulation

Electrons interacting with matter are scattered elastically or inelastically until being effectively absorbed or escaping from the medium of interest.

The average number of collisions that electrons undergo becomes very large for initial energies greater than a few keV and in a medium many mean free paths thick. In such cases Monte Carlo transport calculations apply a "condensed random walk "model. They use multiple scattering theories which allow the simulation of the global electron deflection and energy loss after all collisions occurring in a certain track segment that is much longer than the mean free path (mfp) between the interactions. The accuracy of the condensed methods is thus limited by the approximations in the multiple scattering theories. High energy Monte Carlo codes are for instance ETRAN, EGS and TIGER [15]. They have a lower transport cut-off of 1 keV electron kinetic energy.

For energ less than a few keV the history of each electron can be followed directly from one interaction point to another. The model is classified as "detailed (analog)" Monte Carlo simulation. The accuracy depends on the accuracy of the differential cross sections for individual events and on how precisely the Monte Carlo algorithm used matches the actual interaction processes. Detailed Monte Carlo calculations are applied as a theoretical approach to AES, XPS, for electron track simulation in micro dosimetry, for investigation of the electron reflection from solids etc. The validity of the model is discussed in each particular case. Transport codes for general use are not available to our knowledge.

1.2. Detailed Monte Carlo models of elastic scattering

The investigation of elastic scattering effects requires an adequate description of the electron elastic scattering and an inclusion of total inelastic interaction data without treatment of each inelastic scattering type.

Models applied earlier [1,2,3] contain the following features:

Elastic and inelastic scattering are considered separately. First the electron trajectory through the medium is constructed assuming that the medium has elastic scattering properties only. The probability is then calculated for an electron to pass the simulated total path inside the medium without energy loss. This probability represents the electron contribution to the scored quantities.

The medium is semi-infinite and homogeneous.

The electron escape angle (the angle between the direction of the outgoing electron and the surface normal), the travelled path length or the emission depth (for Auger electrons) are usually monitored.

In this work a detailed Monte Carlo model is described which simulates the transport of elastically scattered electrons through a medium more rigorously. The separate treatment of the elastic and inelastic scattering is avoided.

The electrons travel through a multi layered infinite slab. A semi-infinite homogeneous medium is described as one thick layer.

The electron escape angle, the path length inside the medium, the penetrated depth and the number of suffered elastic scattering events are recorded.

2. DESCRIPTION OF THE MONTE CARLO TRANSPORT MODEL OF ELASTICALLY SCATTERED ELECTRONS

The electron is represented by its position coordinates and direction of motion in a fixed coordinate system. The initial value of these variables is set in accordance with the electron source characteristics: normal or oblique incident electron beam or electrons created inside the material (Auger electrons or photoelectron emission due to X-ray interaction with the matter). The electron energy remains constant during the simulation. The differential elastic cross section data, the elastic and inelastic mfp depend on it.

The trajectory of each electron is constructed as a series of successive interaction events. The distance, s, between (i-1)th and (i)th interaction is sampled from an exponential distribution governed by the total mfp, λ_t:

$$S = -\lambda_t . \log (R) \qquad (1)$$

where:

$$\frac{1}{\lambda_t} = \frac{1}{\lambda_e} + \frac{1}{\lambda_{in}}$$

λ_e and λ_{in} are the elastic and inelastic mfp respectively,

R will always denote a random number uniformly distributed in an interval [0,1]. Any new occurrence of R in the text below will mean a new random number.

The path is rescaled when the electron crosses a boundary between different material layers:

$$S = S_b - \lambda'_t . \log (R) \qquad (2)$$

where S_b is the electron path in the current material and λ'_t is the total mfp for the material entered.

The interaction type is decided by comparison of a random number with the elastic scattering probability:

$$P_e = \frac{\lambda_t}{\lambda_e} \qquad (3)$$

If the collision is elastic, ($R < P_e$), the polar scattering angle, θ, with respect to the direction before collision, is obtained using a direct sampling procedure, i.e. solving the equation:

$$R = \left(\int_0^{\theta} \frac{d\sigma}{d\Omega} d\Omega \right) / \left(\int_0^{\pi} \frac{d\sigma}{d\Omega} d\Omega \right) \qquad (4)$$

where $\frac{d\sigma}{d\Omega}$ is the differential elastic scattering cross section.

(The Monte Carlo code reads the ratios for a fine set of θ-angles as input data.)

The new direction of motion is calculated assuming a uniform distribution of the azimuthal scattering angles.

The electron history is terminated if the collision is inelastic ($R>P_e$). In this way each inelastic event is treated as absorption.

Electrons suffering successive elastic scatterings are followed until they escape from the medium. The electron path lengths in each layer, the maximum penetrated depth and the number of elastic scattering events are updated during the simulation. These values are recorded for each reflected (or transmitted) electron as well as its escape angle. The current contribution of a scored electron is equal to unity.

Thus the angular distribution, the path length and depth distribution and the collision number distribution are obtained simulating the transport of many (10^5-10^6) initial electrons. The statistical uncertainty of the results is estimated from 10 runs of the Monte Carlo code.

3. APPLICATION OF THE MONTE CARLO MODEL

3.1. Reflection coefficient (albedo) from isotropically scattering semi infinite medium

A semi-infinite medium is considered which scatters the electrons isotropically elastically with probability P_e or absorbs them. This was used as a test of the Monte Carlo code since the albedo problem has an analytical solution by Chandrasekhar's theory [4].

The analytical flux, Φ, and the current, J, of the backscattered electrons are expressed as functions of the electron escape angle, μ [5]:

$$\Phi(\mu) = \frac{p_e}{2} \cdot \mu_o \cdot \frac{H(\mu) \cdot H(\mu_o)}{\mu + \mu_o} \tag{5}$$

$$J(\mu) = \mu \Phi(\mu) \tag{6}$$

where μ_o is the cosine of the incident angle of the electrons and $H(\mu)$ is the Chandrasekhar H-function tabulated in [4].

The total half-space current albedo, α, is given analytically by [5]:

$$\alpha = 1 - \sqrt{1 - P_e} \cdot H(\mu_o) \tag{7}$$

Monte Carlo calculations were performed for electrons normally incident on the medium. The elastic scattering probability was varied from 0.1 to 0.95. Isotropic scattering was achieved by sampling of the polar angle by setting:

$$\cos(\theta) = 2.R - 1 \tag{8}$$

The distances are presented in mfp-units, so the input of an explicit total mfp value is not necessary. The angular flux and current distribution of the reflected electrons and the total current albedo are obtained with statistical error less than 1%.

Fig. 1 shows the comparison between the Monte Carlo and the analytical angular distributions of the electron flux and current for μ_o=1 (normal incidence) and for elastic scattering probability P_e = 0.5. The deviations do not exceed the statistical uncertainty. Fig. 2 illusrates the agreement of the analytical total current albedo with the Monte Carlo results for different elastic scattering probabilities.

Thus the test is considered to support the validity of the Monte Carlo code.

3.2. Elastic backscattering from solids: angular distributions

The Monte Carlo model is applied to 1 keV electrons normally incident on aluminium, copper and gold and to 0.4 keV electrons normally incident on silver. The elastic scattering in aluminium, copper and gold is described by Riley's differential cross sections [6]. Fink's data [7] are interpolated to obtain the cross sections for silver. The inelastic mfp is taken from [8].

The angular distribution of the elastically backscattered electrons is calculated with statistical error between 2 and 7% (for the different angle bins).

The results for aluminium and copper are compared with previous published data [3] in Fig. 3a and Fig. 3b. The present data for silver and those from [3] are shown in Fig. 3c. The results for gold are compared with those from [9] in Fig. 3d.

The observed data deviations are considered as acceptable. They may be related mainly to the differences in the cross sections data used.

S_N-calculations of the albedo and the angular distribution for 1 keV electrons on aluminium and gold were performed [10] with the same differential elastic cross sections data and elastic scattering probability as in this work. They agree very well with the present data (see Fig. 4a and 4b).

3.3.Reflection from solids ignoring the inelastic scattering probability: path and depth length distributions

The transport of electrons emitted or backscattered from solids without considerable energy loss (E_0-E<<E_0) is treated in earlier investigations [11,12,13]. A theory of separating the elastic from the inelastic electron interactions, suggested by Tougaard and Sigmund [14], is used to describe the energy spectrum in the vicinity of the primary peak. The probability for an electron to arrive at the solid surface after travelling a certain path length is involved in the expression of the energy distribution. According to the theory this probability is considered to depend on the elastic scattering only ignoring the energy loss processes. The energy spectrum can be then calculated by convoluting the path distribution with the energy loss function but this lies outside the scope of the present paper

The Monte Carlo model is applied to study the influence of the structure of the differential elastic scattering cross section on the electron path inside the medium, on the penetrated depth and the number of suffered collisions by the reflected electrons.

3.3.1. The Monte Carlo model within the Tougaard-Sigmund theory.

The Tougaard-Sigmund approach is included in the Monte Carlo model by stating that the inelastic mfp is much larger than the elastic mfp. The total mfp becomes equal to the elastic mfp and the elastic scattering probability is unity (see chap.2).

The electron scattering is simulated until the electron escapes from the surface of the semi-infinite medium or its path length exceeds a certain value.

The differential elastic scattering cross sections used are taken (or interpolated) from Riley's and Fink's data [6,7].

3.3.2. Results for a normally incident electron beam.

Monte Carlo calculations were performed for the reflection of 1 keV and 20 keV electrons from aluminium, 1 keV and 4 keV electrons from copper, 0.5 keV and 1 keV electrons from carbon, 1.32 keV electrons from sulphur, 0.5 keV electrons from titanium and 0.4 keV electrons from silver (short notation - Ag(0.4 keV)). The statistical error is about 1-3%.

The results are separated into two groups corresponding to the different behaviour of the path length, depth, and collision number distribution obtained.

The first group contains cases for which the distributions are monotonously decreasing: Cu (1 keV); Ti (0.5 keV) and Ag (0.4 keV) - see Fig 5a and 5b.

The other cases listed above, namely Al (1 keV), Al (20 keV), Cu (4 keV), C (0.5 keV), C (1 keV) and S (1.32 keV), belong to the second group for which the distributions have a maximum in the initial region and then decrease monotonously - Fig. 6a to 6f. It is interesting to note that the case of Al (1 keV) was treated by Tofterup [11] in the P_1 approximation but his results were monotonous. The P_1 approximation is incapable to reconstruct either the non-monotonous character of the solution or the correct angular dependence of the reflected electrons (see also the comments in [3]). An analysis of the problem with the double P_1 approximation will be presented in [16].

Most of the reflected electrons tend to penetrate a depth about 3.3 times shorter than the most probable electron path inside the medium. Furthermore the maximum number of collisions suffered by the reflected electrons corresponds to the most probable path length in mfp units (as should be expected). So the three distributions are related by one and the same manner for each case of the second group.

The reflection of 1 keV electrons from aluminium and copper is investigated in more detail. The depth distribution of electrons backscattered

after a fixed collision number was calculated. Fig. 7a and Fig. 7b show the plot of the results for aluminium and copper respectively. Electrons which have suffered one and two interactions are reflected from the surface. They have a monotonic depth distribution. A maximum appears for electrons with three interactions. The electrons penetrate deeper into the medium when the collision number is increased (the maximum moves to larger depth lengths). The probability of the electron to be reflected from aluminium becomes smaller after about ten collision (the area under the depth distributions decreases). In contrast to that, electrons suffering one and two collisions comprise the major fraction of the electrons backscattered from copper.

Discussion

It is interesting to investigate which properties of the differential elastic scattering cross section can be attributed to the non-monotonic character of the path and depth length distributions.

Analysing the results from both groups it is found that the presence of a maximum in the distributions and its location depends strongly on the backscattering probability, P_b, for a single scattering event:

$$P_b = \left(\int_{\pi/2}^{\pi} \frac{d\sigma}{d\Omega} d\Omega \right) / \left(\int_{0}^{\pi} \frac{d\sigma}{d\Omega} d\Omega \right) \qquad (9)$$

The position of the maximum in the depth length distribution is used to illustrate this dependence on Fig (8) since this maximum is better pronounced.

It is seen that a non-monotonic behaviour of the distributions exists if the backscattering probability is less than about 4.10^{-2}.

Another observation is that the differential elastic scattering cross sections for all cases in the second group are decreasing functions of the polar scattering angle over the whole interval [0, 2π]. This appears to imply that another condition for the existence of non monotonic distributions is that the scattering cross section must be a monotonously decreasing function of the scattering angle. This is illustrated with the case of Ti (0.5 keV). The backscattering probability for the Ti (0.5 keV) case is 0.02 (value smaller than that of Al (1 keV)) but the differential elastic scattering cross section increases for the largest scattering angles. Monotonic distributions were obtained (already shown on Fig. 5b)

The relation of the most probable penetrated depth and the path length obviously rely on the structure of the elastic scattering cross sections but a detailed explanation is not suggested here.

3.3.3. Results for an oblique incident electron beam.

Path and depth length distributions of 1 keV electrons reflected from aluminium were calculated for an oblique incident electron beam. The incident angle, α_{in}, is defined with respect to the surface normal. The results for $\cos(\alpha_{in}) = 0.4$, 0.6 and 0.8 as well as for a normal incidence are plotted on Fig. 9a and 9b. As expected, the distributions become more and more concentrated towards the surface with increasing angle if incidence. The path and depth maxima locations may be related to those for a normal incident electron beam as follows:

$$P_{0b} = \cos(\alpha_{in}).P_{ni} \qquad (10)$$
$$D_{0b} = \cos(\alpha_{in}).D_{ni}$$

Here P_{0b} is the position of the maximum in the path length distribution for an oblique incident electron beam. The meaning of the other notations is self explaining.

A simplified interpretation may be stated as most of the electrons pass one and the same distance ("effective depth") along the direction of incidence. The effective depth coincides with the penetrated material thickness for the normal incidence case.

4.CONCLUSION

The Monte Carlo method presented was applied successfully to study the electron elastic backscattering from a semi-infinite homogeneous medium. The accuracy of the results can be improved by inclusion of more precise differential elastic scattering cross sections and mean free path data. It is advisable for instance to avoid the interpolation of Fink's cross sections since the step in the selected energies is large. Furthermore, it is necessary to take into account the exchange and charge cloud polarization effects.

The problems considered do not use the whole potential of the Monte Carlo code (the capability to simulate different electron sources, to treat layered medium or to estimate the electron transmission).

A CM FORTRAN version of the Monte Carlo code and its run on a Connection Machine System are under preparation.

Acknowledgments

This work was made possible through a postdoc fellowship granted within the East European Research Program of Chalmers University of Technology.

I would like to thank Prof. Imre Pazsit for the introduction into the subject. His constant encouragement with many helpful discussions and suggestions are gratefully acknowledged. I am indebted also to Profs.N.G.-Sjösrand and A.K.Prinja for their constructive and stimulating discussions. I am grateful to Dr. N.S.Garis for his help and the shown interest.

Ing. L. Norberg is also acknowledged for his technical support regarding the SUN-SPARC station.

References

1. A. Jablonski, Elastic backscattering of electrons from surfaces, Surf. Sci., 151 (1985) 166

2. A. Jablonski, Effects of Auger electron elastic scattering in quantitative AES, Surf. Sci.,188 (1987) 164

3. A. Jablonski, Elastic electron backscattering from surfaces, Phys.-Rev. B, 39 (1989) 61

4. S. Chandrasekhar, Radiative transfer, Dover, New York, 1960

5. A. Prinja (1994), private communication

6. M. Riley, G.J.MacCallum and F.Biggs, Theoretical electron-atom elastic scattering cross sections, At. Data and Nucl. Data Tables, 15 (1975) 443

7. G. Fink, Theoretical electron scattering amplitudes and spin polarisation, At. Data and Nucl. Data Tables, 14 (1974) 39

8. S. Tanuma, C. Powell and D. Penn, Calculations of electron inelastic mean free paths, Surface and Interface Analysis, 17 (1991) 911

9. A.Jablonski, Elastic electron backscattering from gold, Phys. Rev. B, 43 (1991) 7546

10. N.G. Sjöstrand, Numerical study of electron scattering, CTH-RF-102, 1994

11. A. Tofterup, Elastic and inelastic scattering of electrons reflected from solids: effects on energy spectra, Phys. Rev. B 32 (1985) 2808

12. A. Tofterup, Depth profiling through quantitative analysis of energy spectra in XPS and AES: analytical formalism, Surf. Sci., 248 (1991) 77

13. L. Tilinin and W. Werner, Angular and energy distribution of Auger and photoelectrons escaping from non crystalline solid surfaces Surf. Sci., 290 (1993) 119

14. S. Tougaard and P. Sigmund, Influence of elastic and inelastic scattering on energy spectra of electrons emitted from solids, Phys. Rev. B, 25 (1982) 4452

15. T.M.Jenkins, W.R. Nelson, A. Rindi, Monte Carlo transport of electrons and photons, Ettore Majorana International Science Series Vol. 38, New York, Plenum Press, 1988

16. I.Pazsit and R. Chakarova, The path and depth length distribution of electrons reflected from solids, in preparation

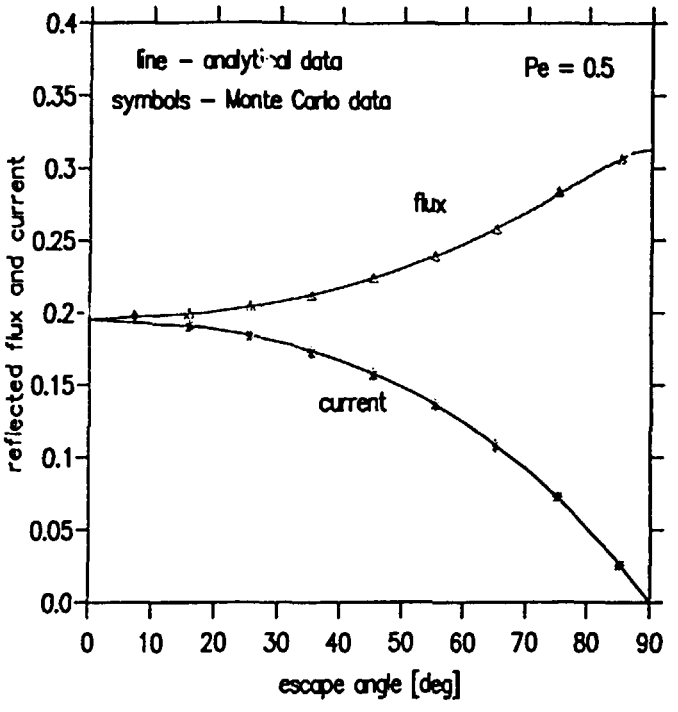

Fig. 1 Angular flux and current distribution of electrons reflected from an isotropically scattering medium. Comparison between the analytical data according to the Chandrasekhar theory and Monte Carlo data. The elastic scattering probability is 0.5.

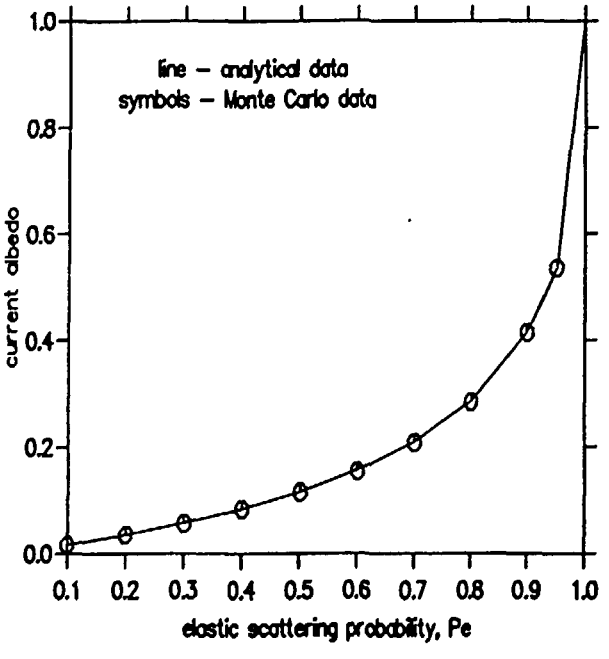

Fig. 2 Total half space albedo for an isotropically scattering medium for different elastic scattering probabilities. Comparison between the analytical data according to the Chandrasekhar theory and the Monte Carlo data.

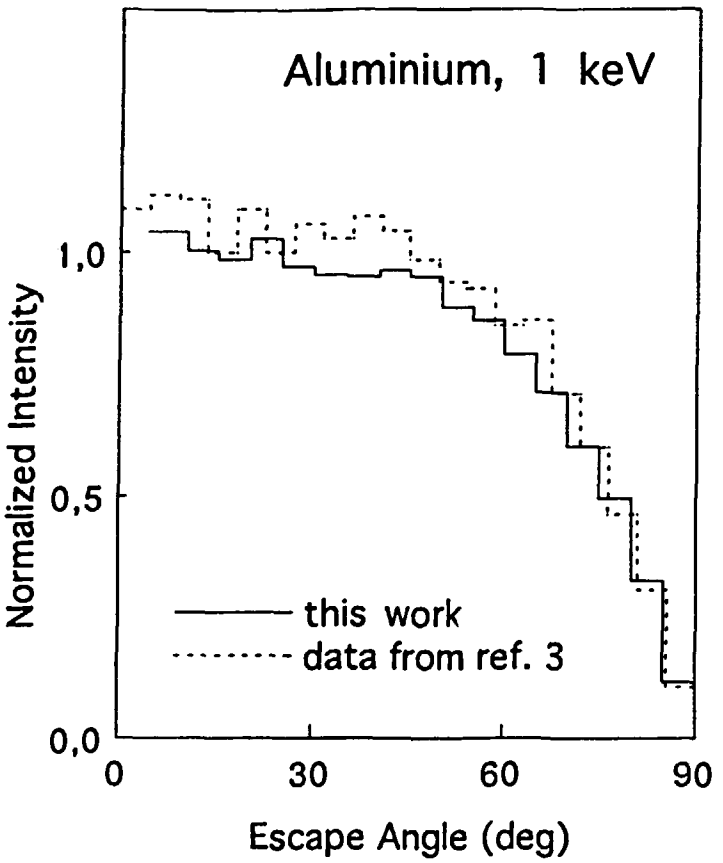

Fig. 3 Angular distribution of elastically backscattered electrons - comparison of the calculated data and those from [3]:
(a) 1 keV electrons reflected from aluminium

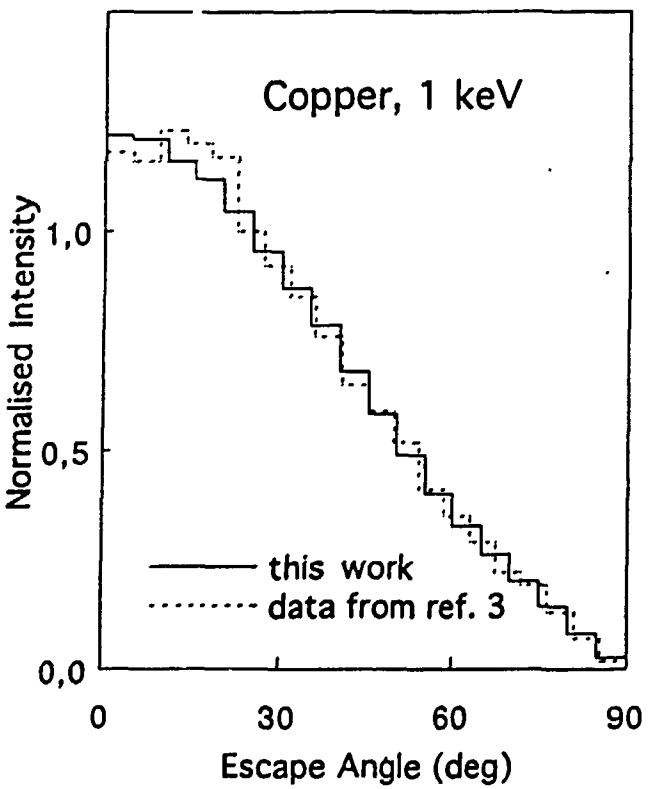

Fig. 3 continues:
(b) 1 keV electrons reflected from copper

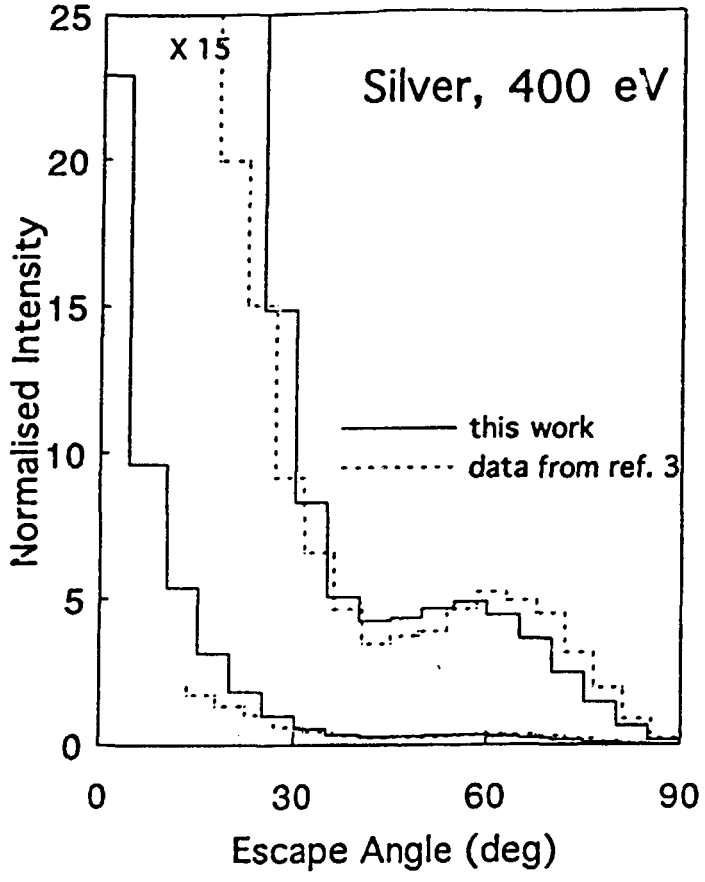

Fig. 3 continues:
(c) 0.4 keV electrons reflected from silver

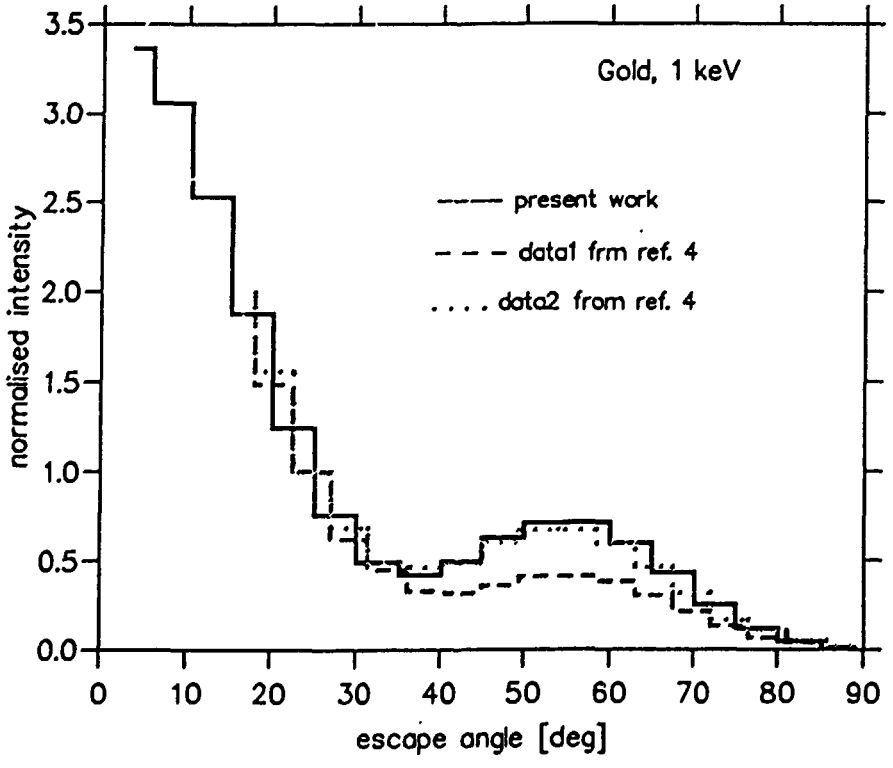

Fig. 3 continues:
(d) 1 keV electrons reflected from gold.

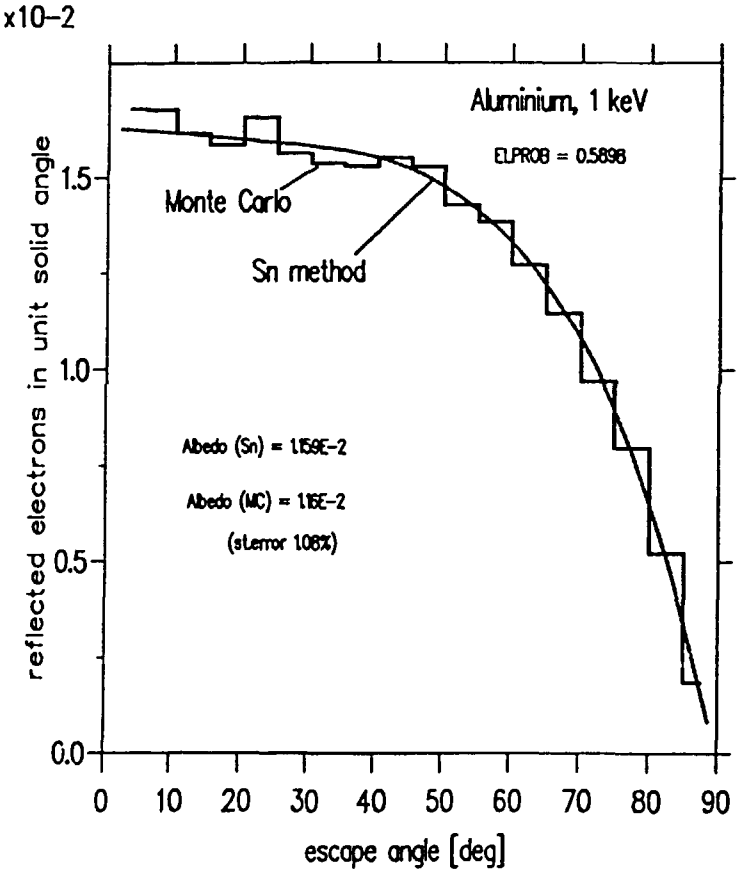

Fig.4a Angular distribution of 1 keV elastically backscattered electrons from aluminium. Comparison between the calculated data and those from [9].

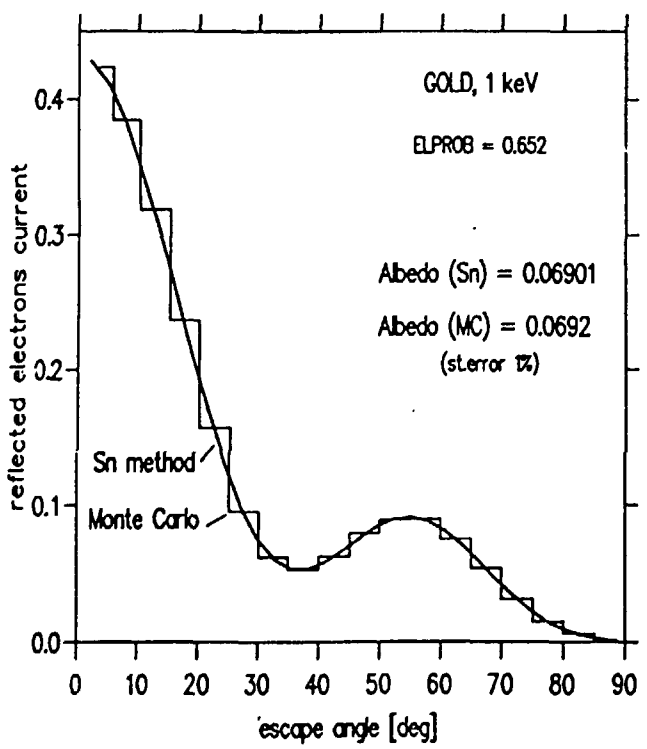

Fig.4b Angular distribution of 1 keV elastically backscattered electrons from gold. Comparison between the calculated data and those from [9].

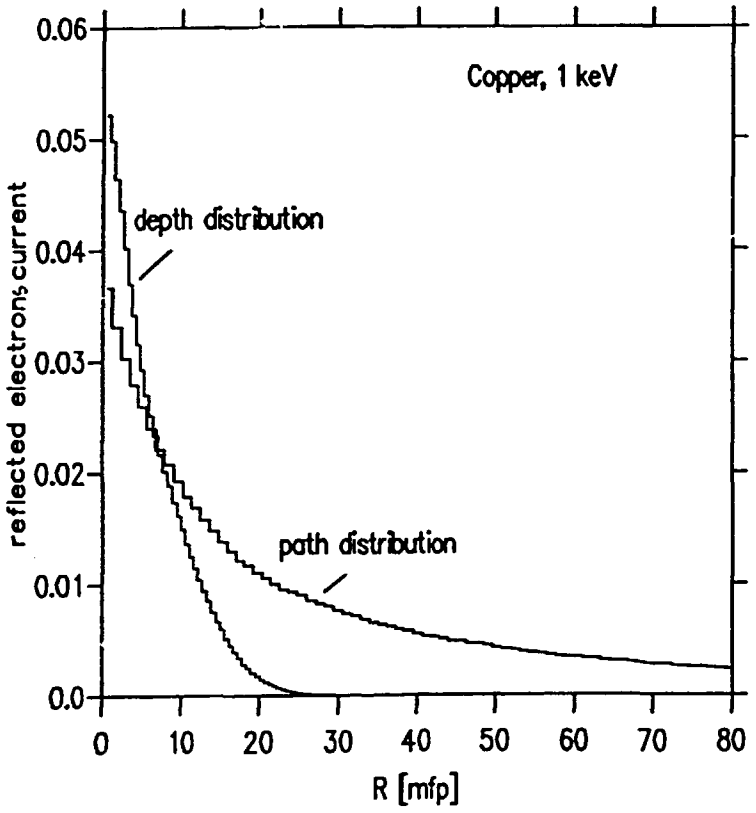

Fig. 5 Path and depth length distribution of the reflected electrons normally incident on a perfect elastically scattering medium:
(a) 1 keV electrons reflected from copper

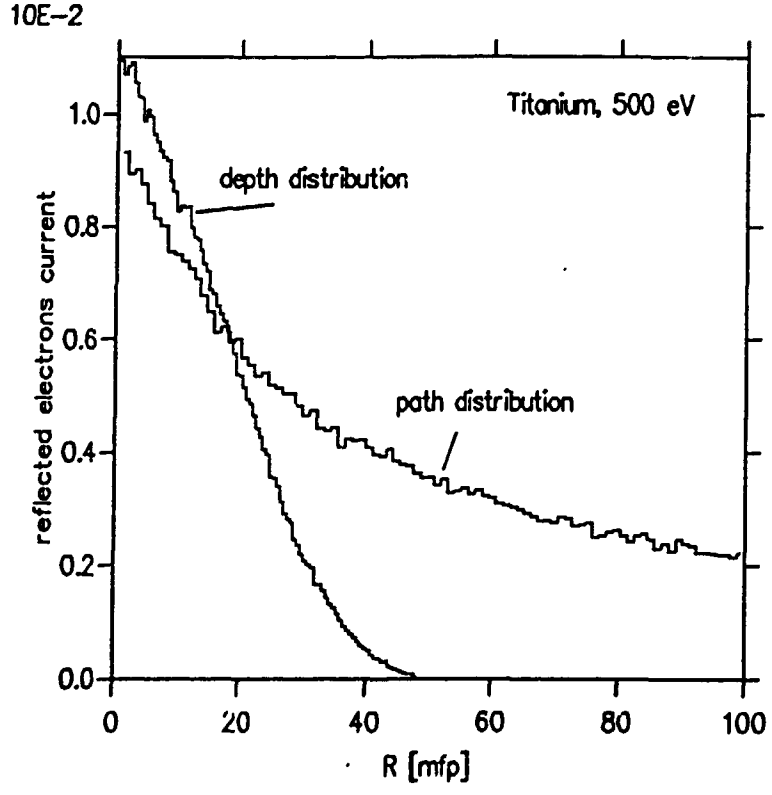

Fig. 5 continues:
(b) 0.5 keV electrons reflected from titanium.

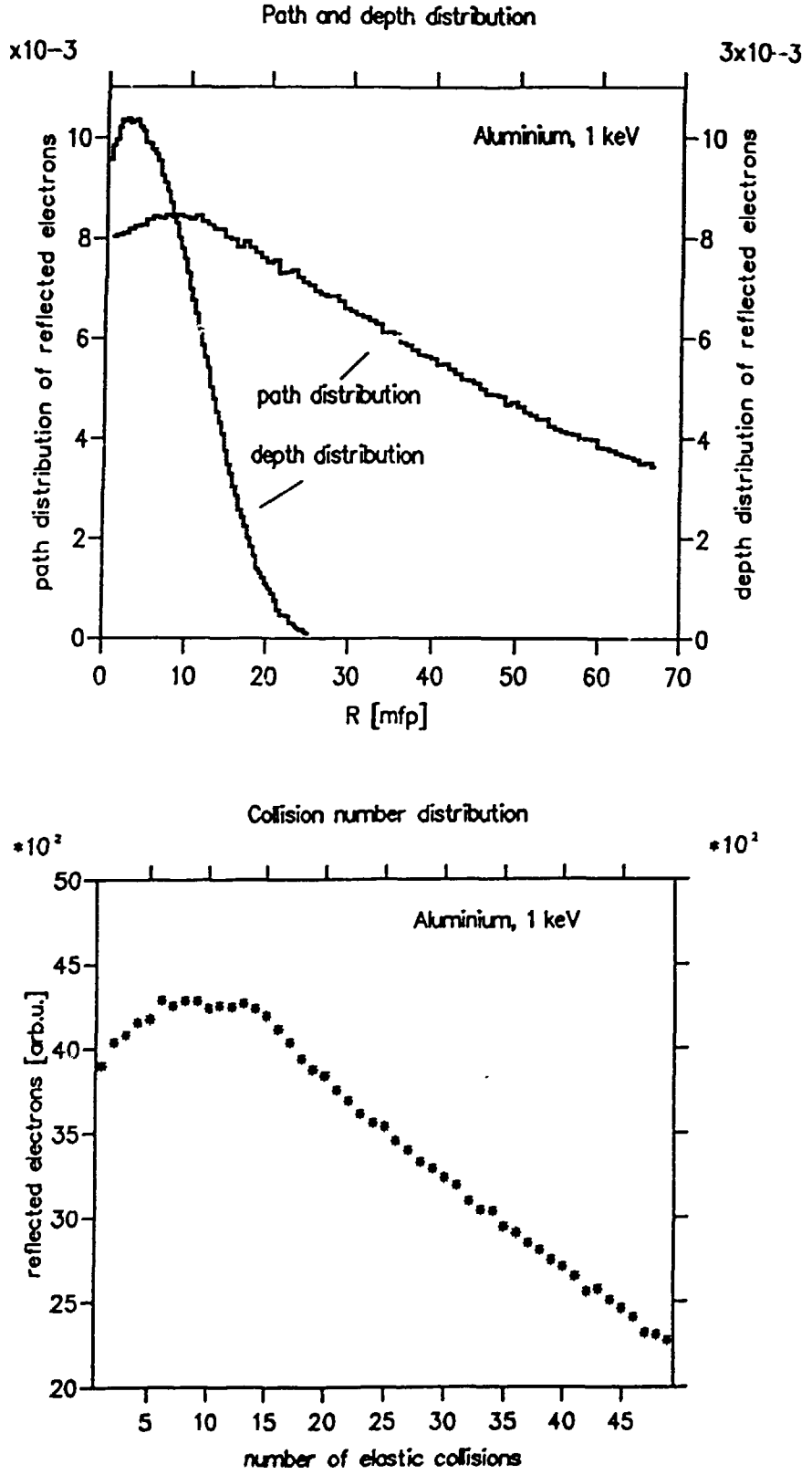

Fig. 6 Path, depth length and collision number distribution of the reflected electrons normally incident on a perfect elastically scattering medium:
(a) 1 keV electrons on aluminium

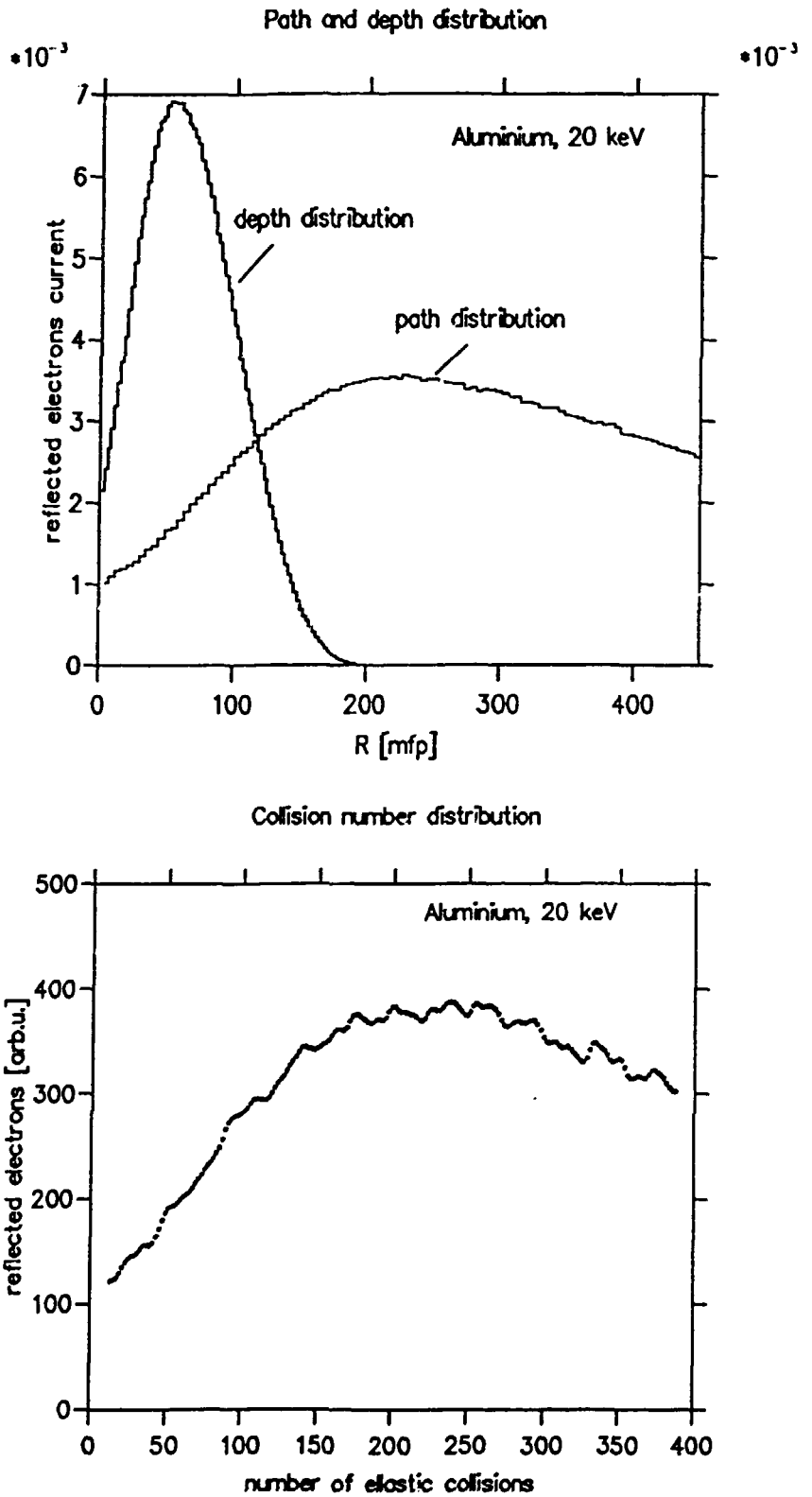

Fig. 6 continues:
(b) 20 keV electrons on aluminium

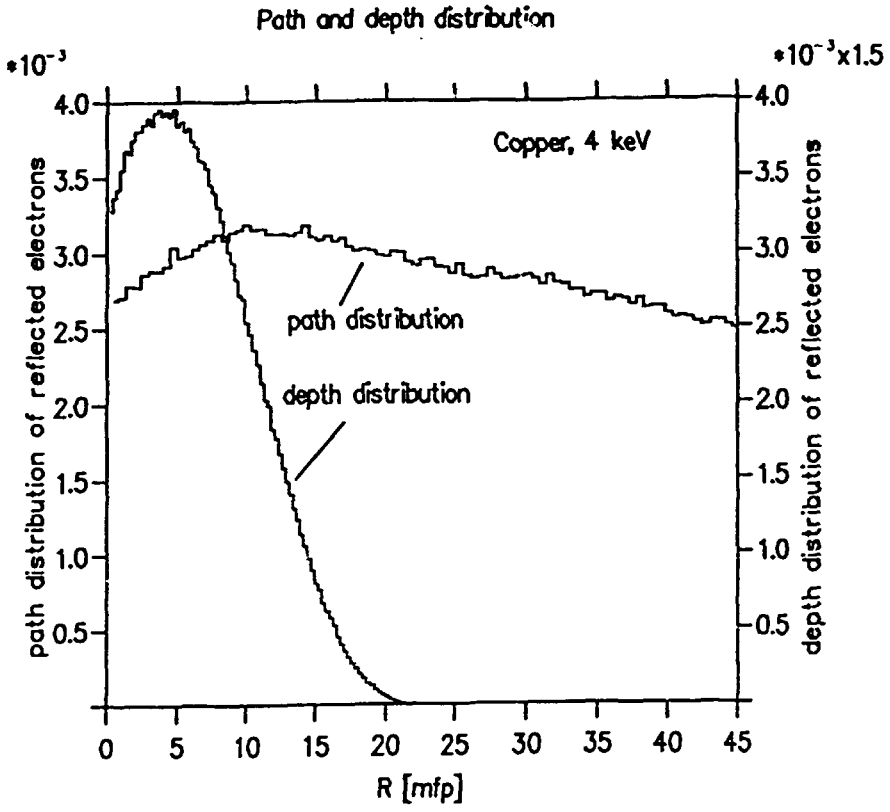

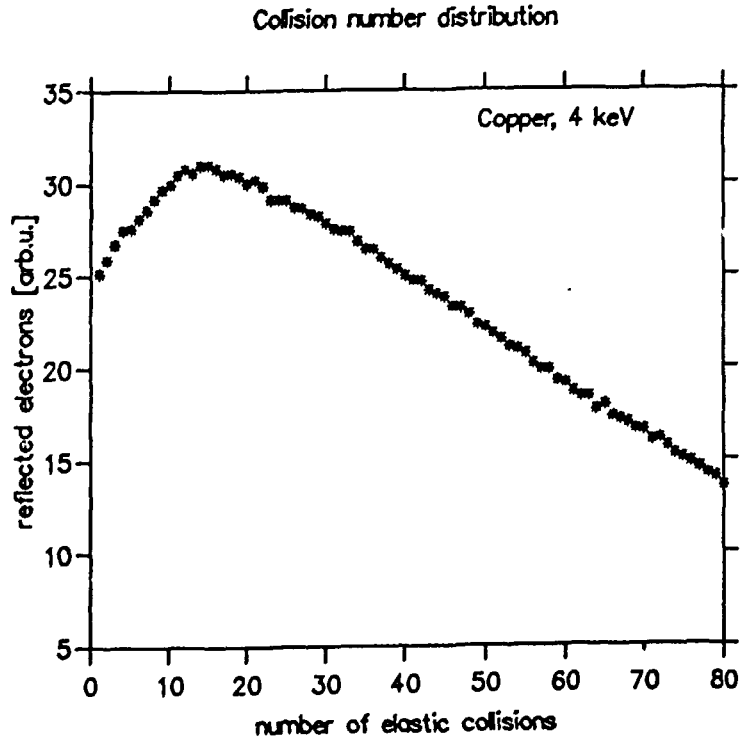

Fig. 6 continues:
(c) 4 keV electrons on copper

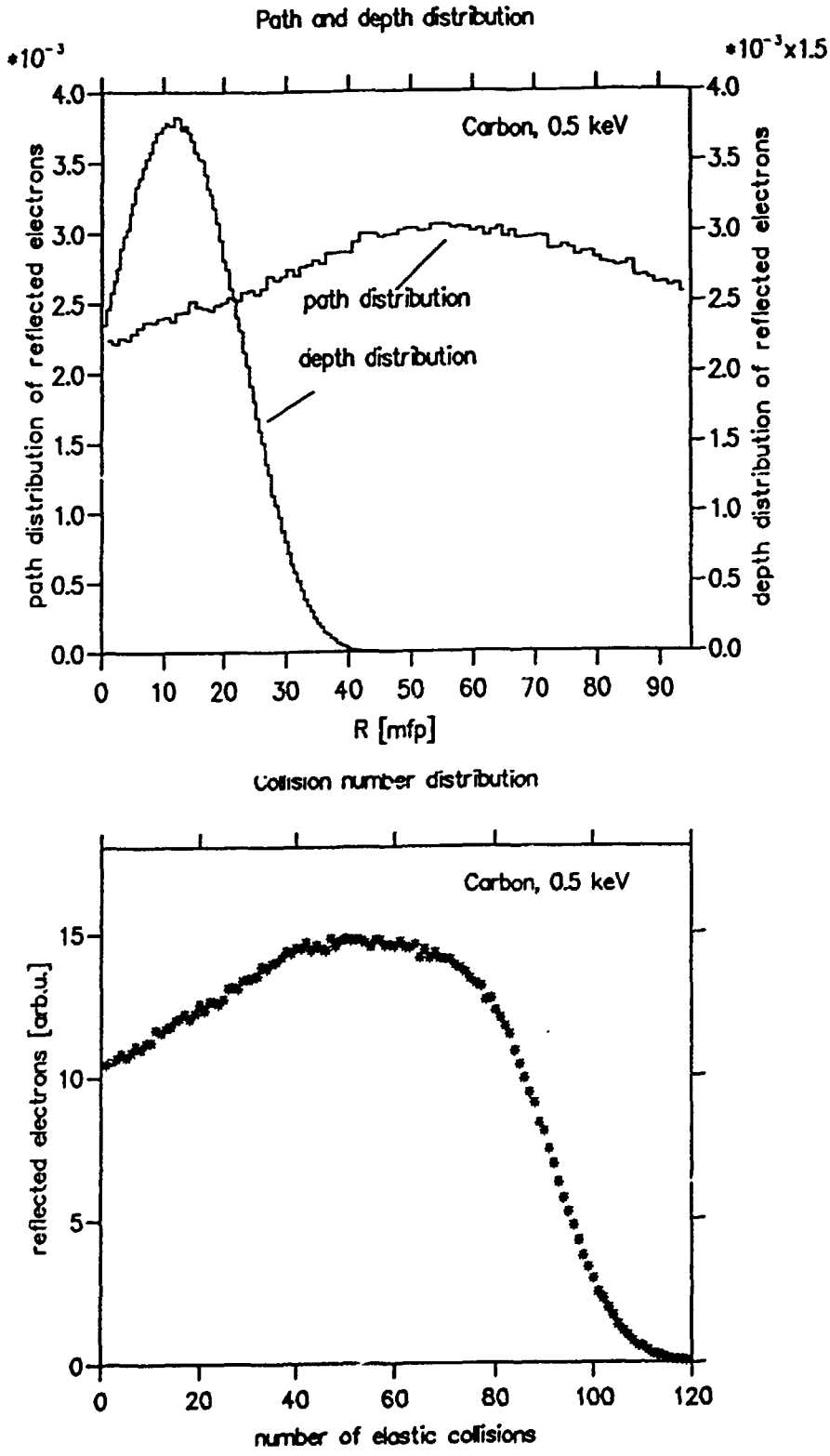

Fig. 6 continues:
(d) 0.5 keV electrons on carbon

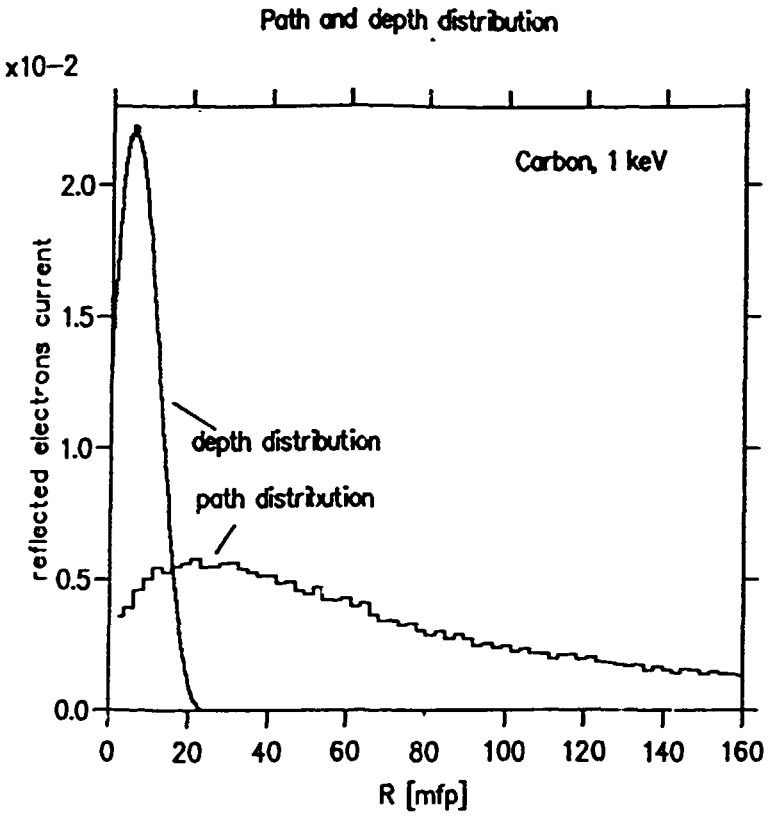

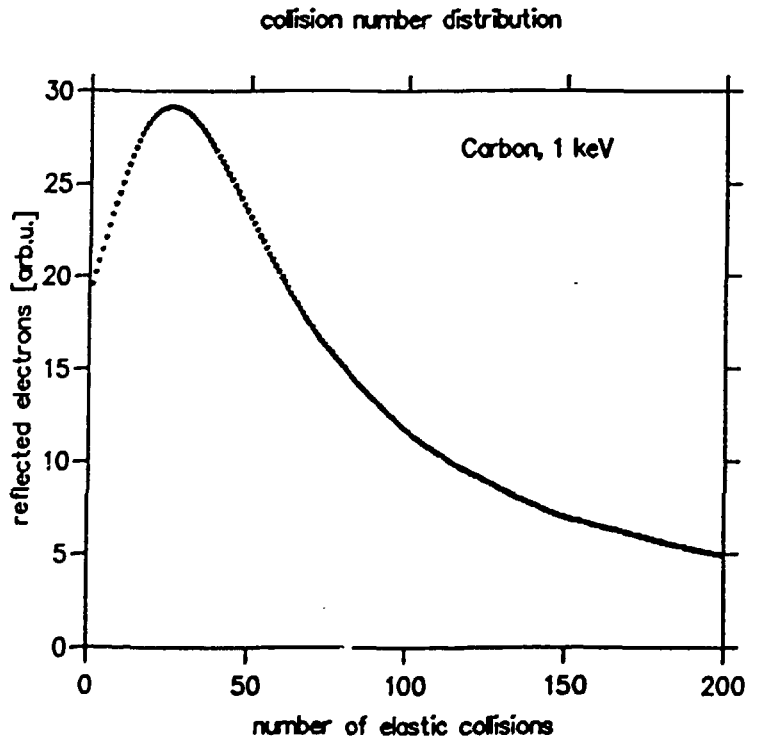

Fig. 6 continues:
(e) 1 keV electrons on carbon

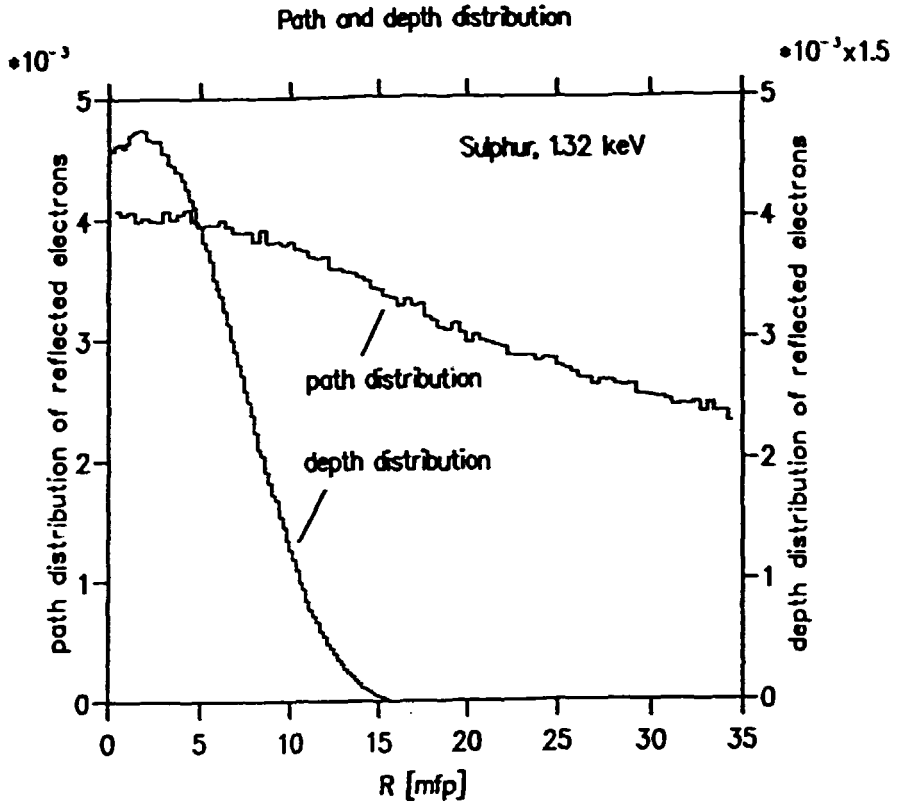

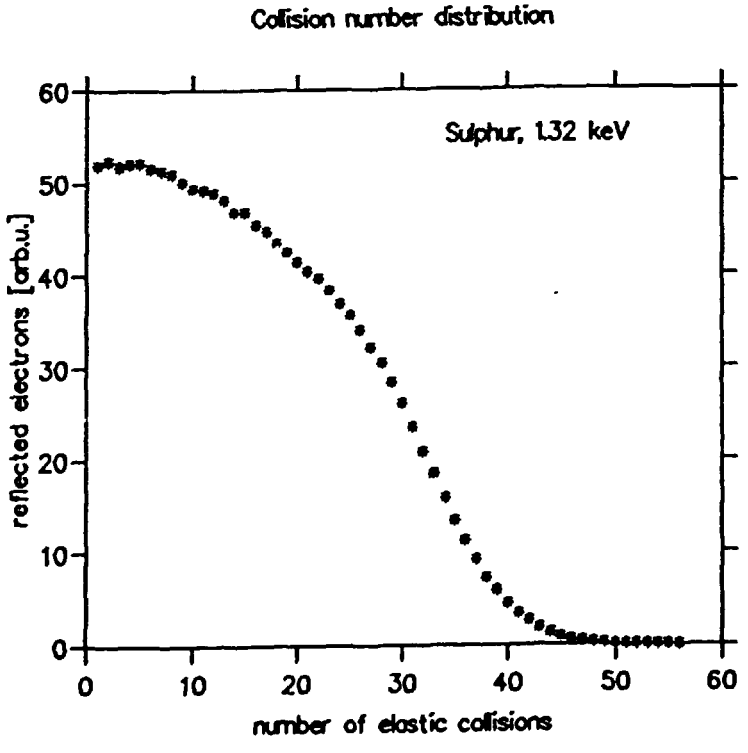

Fig. 6 continues:
(f) 1.32 keV electrons on sulphur

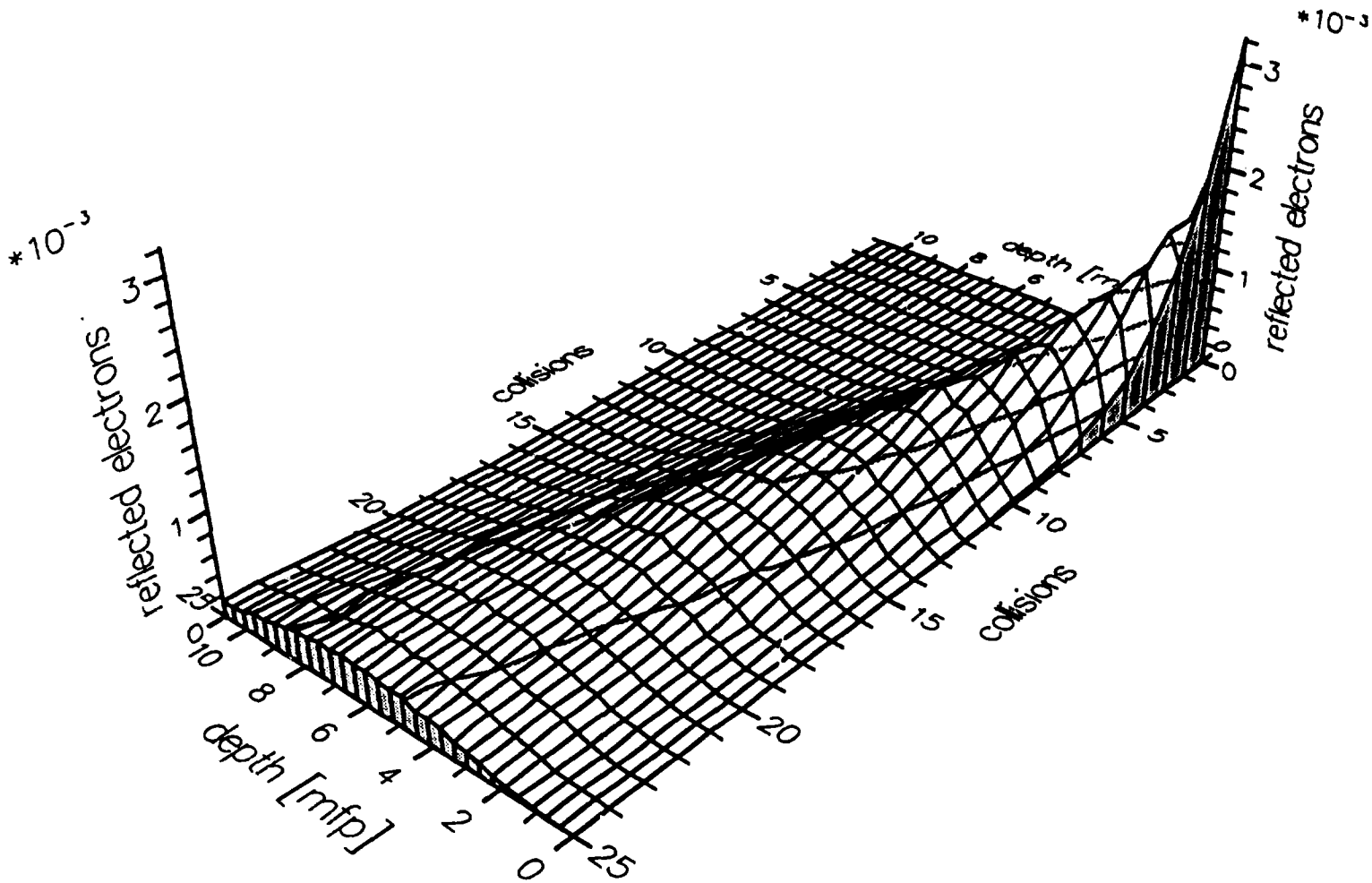

Fig. 7a Depth distribution of 1 keV electrons reflected from aluminium after a fixed number of collisions

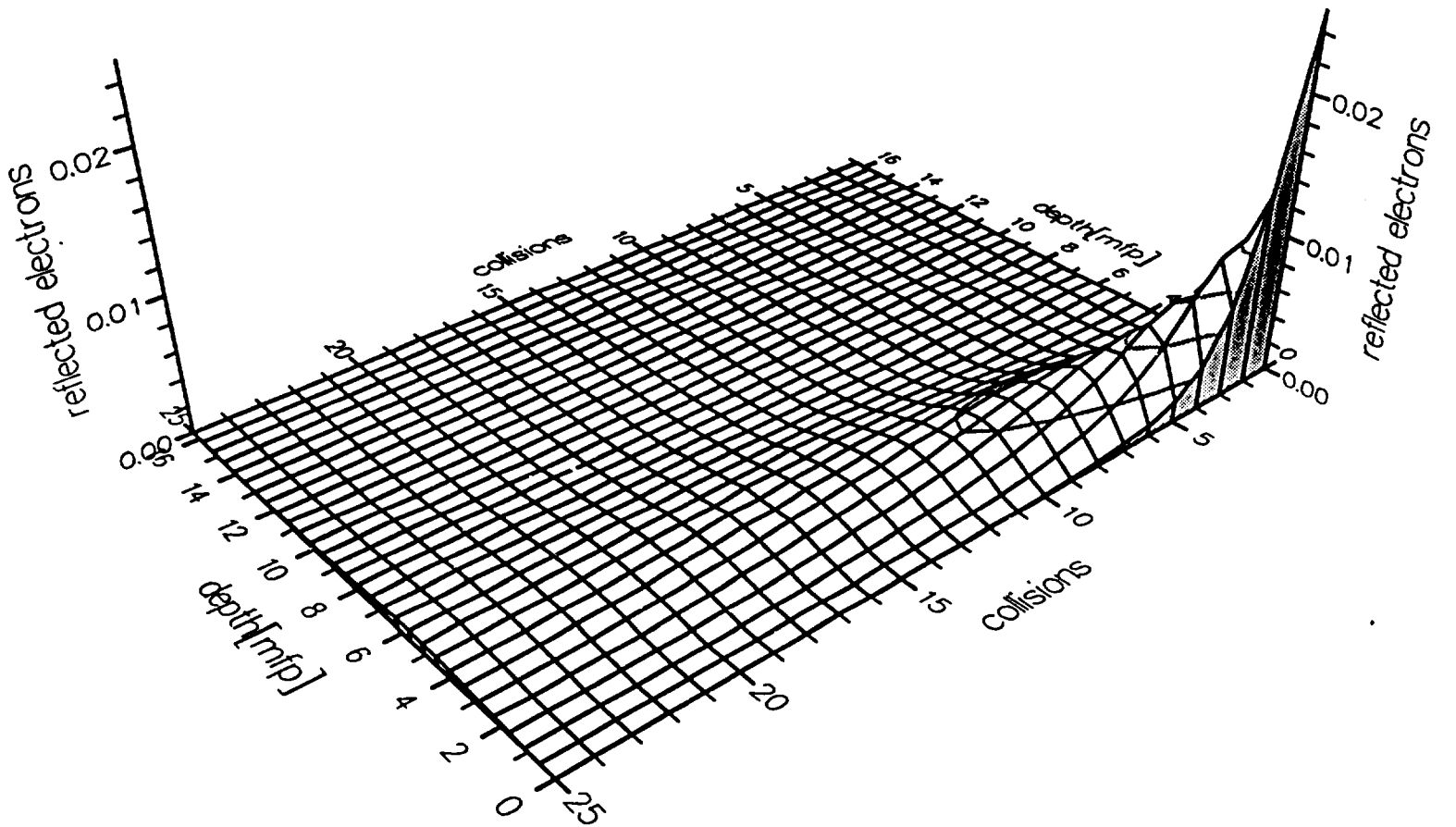

Fig. 7b Depth distribution of 1 keV electrons reflected from copper after a fixed number of collisions

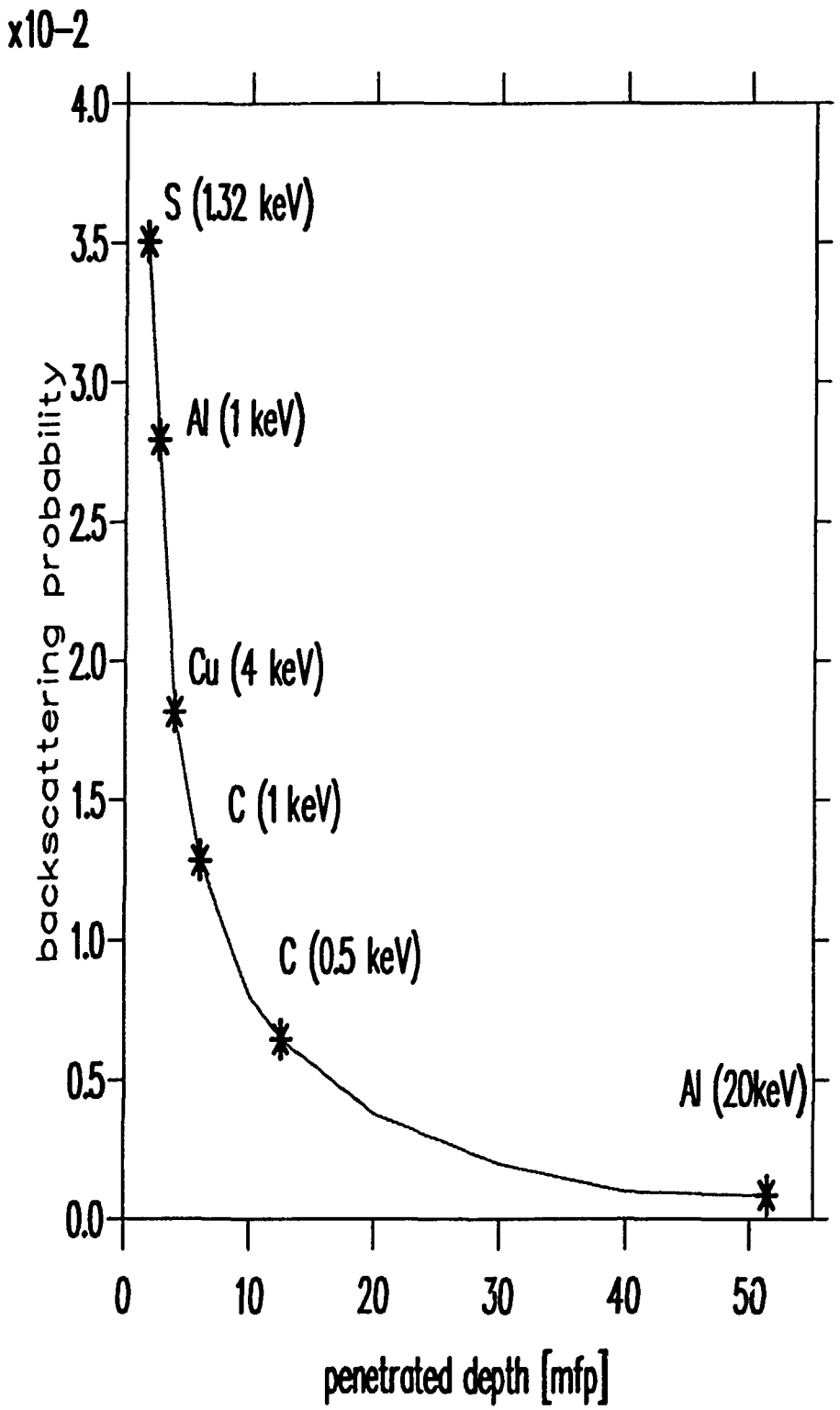

Fig. 8 The backscattering probability for a single scattering event as a function of the most probable penetrated depth by the electrons before being reflected.

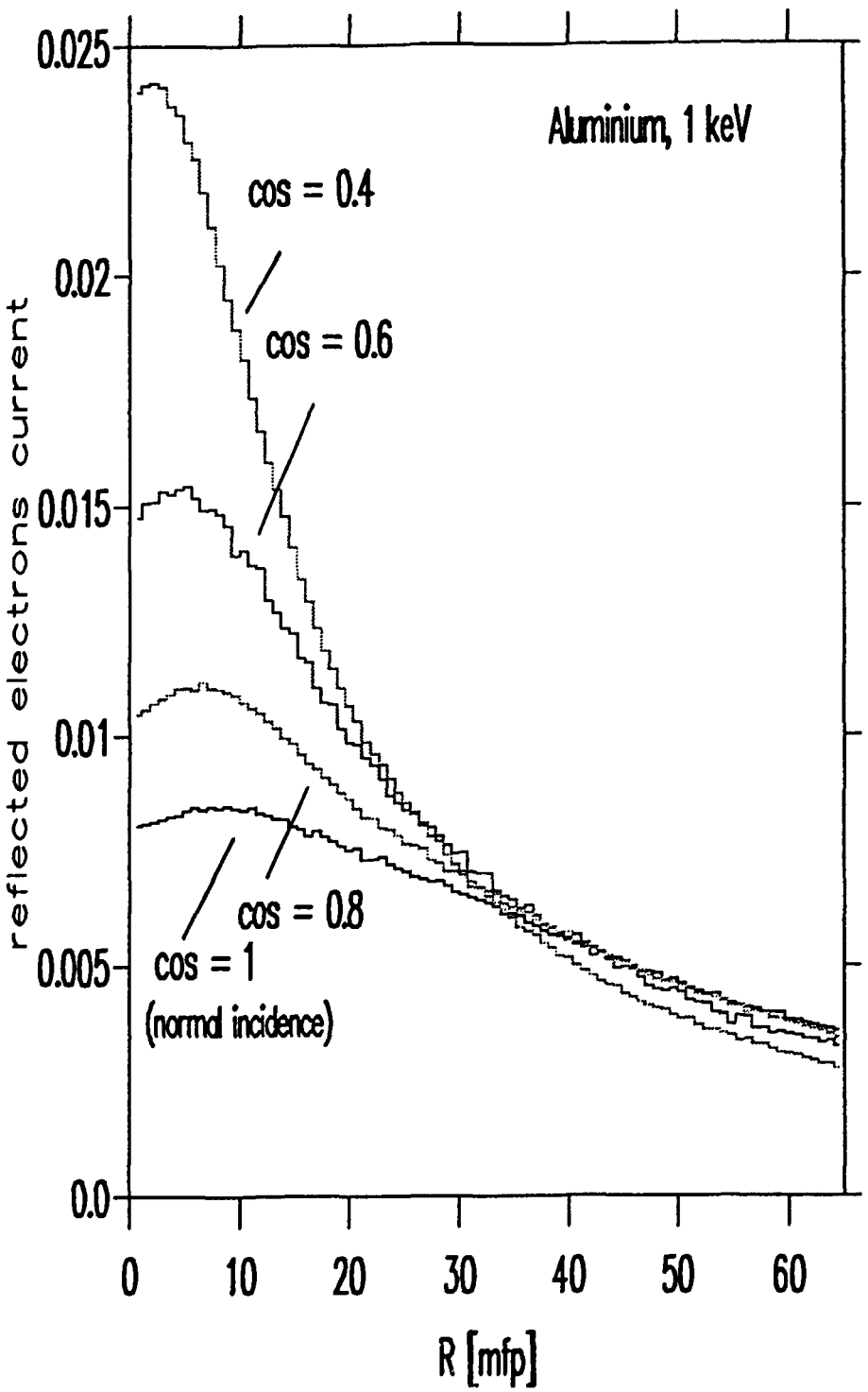

Fig. 9 Reflection of 1 keV electrons normally and obliquely incident on aluminium:

(a) path distribution

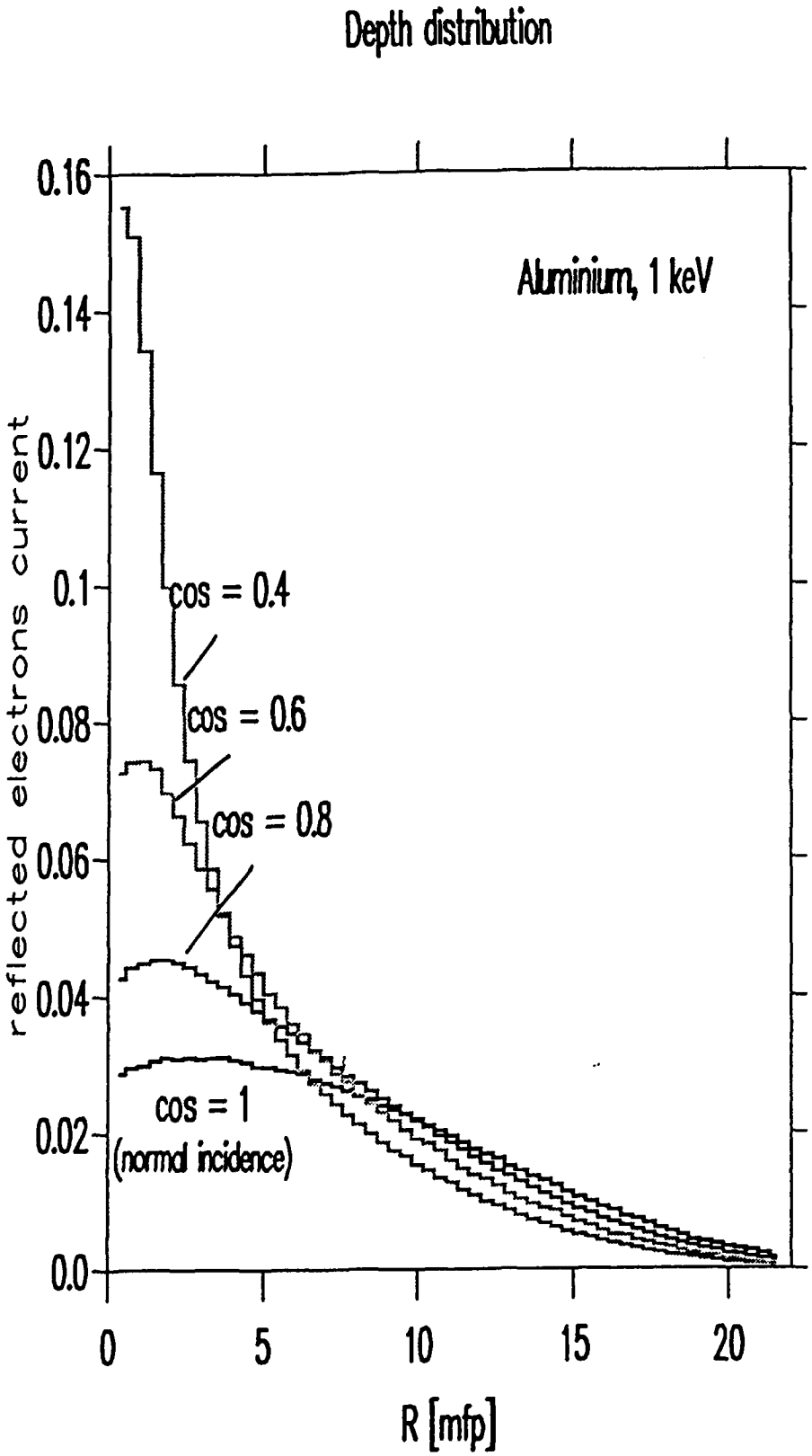

Fig. 9 continues:
(b) depth length distribution